

## Full Paper

# Carbon Nanotubes Based Nanoelectrode Arrays: Fabrication, Evaluation, and Application in Voltammetric Analysis

Yi Tu,<sup>a</sup> Yuehe Lin,<sup>\*b</sup> Wassana Yantasee,<sup>b</sup> Zhifeng Ren<sup>a</sup>

<sup>a</sup> Boston College, Chestnut Hill, Massachusetts, 02467, USA

<sup>b</sup> Pacific Northwest National Laboratory, 902 Battelle Boulevard, Richland, Washington, 99352, USA

\*e-mail: Yuehe.lin@pnl.gov

Received: April 21, 2004

Final version: May 24, 2004

## Abstract

Fabrication, electrochemical characterization, and applications of *low-site density* carbon nanotubes based nanoelectrode arrays (CNTs-NEAs) are reported in this work. Spin-coating of an epoxy resin provides a new way to create the electrode passivation layer effectively reducing electrode capacitance and current leakage. Cyclic voltammetry showed the sigmoidal shape curves with low capacitive current and scan-rate-independent limiting current. Square-wave voltammetry showed well-defined peak shapes in voltammograms of  $K_3Fe(CN)_6$  and 4-acetamidophenol (acetaminophen) and the peak currents to be proportioned to their concentrations, demonstrating the feasibility for voltammetric analysis of the CNTs-NEAs. The CNTs-NEAs were also used successfully for voltammetric detection of trace concentrations of lead(II) at ppb level at first-time. The CNTs-NEAs provide an excellent platform for ultra sensitive electrochemical sensors for chemical and biological sensing.

**Keywords:** Carbon-nanotubes, Nanoelectrode arrays, Voltammetry, Lead

## 1. Introduction

Carbon has been widely used as an electrode material because it has many advantages, including good electrical conductivity, chemically inert, and wide potential range. Carbon nanotubes (CNTs), as a novel form of carbon, have been studied for their electrochemical behaviors [1–11]. It was found that CNTs have many interesting properties such as fast electron transfer rate [6] and high electrocatalytic activity [7, 8]. In addition, CNTs can be functionalized with different bio-molecules such as DNA and protein [12–15]. Based on these unique properties, several research groups have demonstrated that bundle of CNTs [2, 12], CNTs membrane [3], polymer-CNTs composite [7] and CNTs modified electrodes [10, 14, 16] can be used as effective electrochemical biosensors. The previous work, however, takes advantage of the bulk properties of CNTs. Our work explores another important feature of CNT, which is its ultra small size, that can be very useful in making nanoelectrode.

The nanoelectrode has high mass sensitivity, increased mass transport rate and decreased influence of the solution resistance. Sigmoidal voltammograms have been obtained by using single CNT as nanoelectrode [9]. Using multiple CNTs that were properly constructed into certain architecture, researchers were able to fabricate nanoelectrode arrays (NEAs) [17–19]. The array of nanoelectrodes can produce a much higher current than a single nanoelectrode, which can avoid the need for expensive electronic devices and improve the signal to noise ratio. The NEAs have more practical values as ultrasensitive electrochemical sensors for chemical and biological sensing.

In the fabrication of nanoelectrode arrays, certain important requirements should be met. First, the inter-spacing of the individual electrodes should be much larger than the radius of each electrode; otherwise the closely packed nanoelectrode array will behave similar to a macroelectrode due to the diffusion layer overlap [19–23]. Second, there must be a sufficient passivation layer that can protect the underlying conducting layer as well as prevent current leakage and corrosion. Both inorganic materials, such as  $SiO_2$ ,  $Si_3N_4$ , and organic materials, such as epoxy, and photo resist, have been previously tested [24]. The ideal passivation layer is captive and crack-free, long lasting in aqueous electrolyte solutions, good adhesion to substrates and electrodes, mechanically strong, and easy-processing. CNT forest electrodes have been reported for biosensor application recently [25]. The CNT forest electrodes reported did not act as individual nanoelectrodes because of high-density of the CNT forest.

In our previous report [17], we demonstrated the fabrication of nanoelectrode array based on low-site density aligned carbon nanotubes. Controlled low-site density of aligned CNTs is the key for fabrication of CNTs-NEAs. Vertical aligned CNTs produced by plasma-enhanced chemical vapor deposition provide a well-defined architecture for the fabrication of NEAs; the site density of the aligned CNTs can be controlled by tuning the site density of Ni nanoparticles, which serve as catalysts, using electrochemical deposition method [26]. The inter-electrode spacing can be as large as several micrometer that met the requirement, but the insulation material tested in the previous attempt was not good enough to prevent the

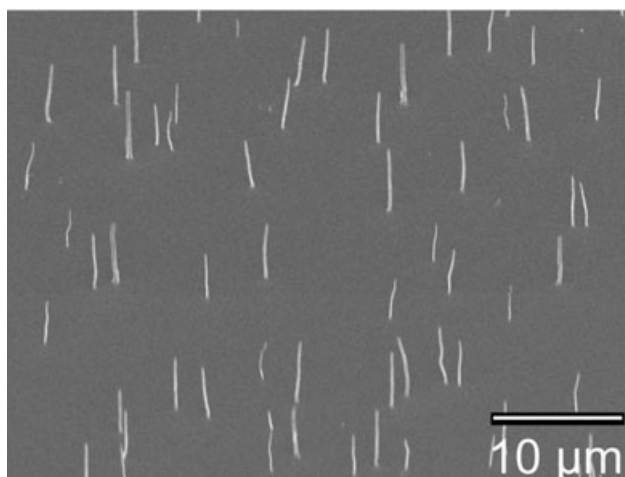


Fig. 1. SEM image of aligned CNT arrays with site density of  $2 \times 10^6 \text{ cm}^{-2}$ .

current leakage, which resulted in the distortion of the cyclic voltammetry curve.

Recently, we have been trying to improve the fabrication method using better insulating materials and packing procedures that solve the leakage problem plus a pretreatment of the electrode to reduce the peak separation. As a result, the excellent sigmoidal shape cyclic voltammogram behavior is obtained on the nanoelectrode array. The details of the fabrication and evaluation of the carbon nanotubes nanoelectrode arrays by using cyclic voltammetry and square-wave voltammetry are presented in this report. The application of using this nanoelectrode arrays in stripping analysis of trace amount of lead(II) ion is also discussed. This is the first report on using CNTs-NEAs for metal ion detection based on stripping voltammetry.

## 2. Experimental

### 2.1. Chemicals

Epon epoxy resin 828 and curing agent *m*-phenylenediamine (MPDA) were from Miller-Stephenson Chemical Company, Inc (Danbury, CT, USA). Other chemicals were from Sigma-Aldrich (St. Louis, MO, USA). Deionized (DI) water was from a Millipore Milli-Q water purification system (Billerica, MA, USA). The metal ion solutions were prepared daily by dilution of the atomic absorption standard solutions with DI water.

### 2.2. Fabrication of Carbon Nanotubes Nanoelectrode Arrays

Ni nanoparticles were first electrodeposited on a Cr-coated Si substrate with the area of  $1 \text{ cm}^2$ . The aligned CNTs arrays with low site density were subsequently grown from those Ni nanoparticles by plasma enhanced chemical vapor deposition [26]. The aligned CNTs arrays had a site density of  $1 \times$

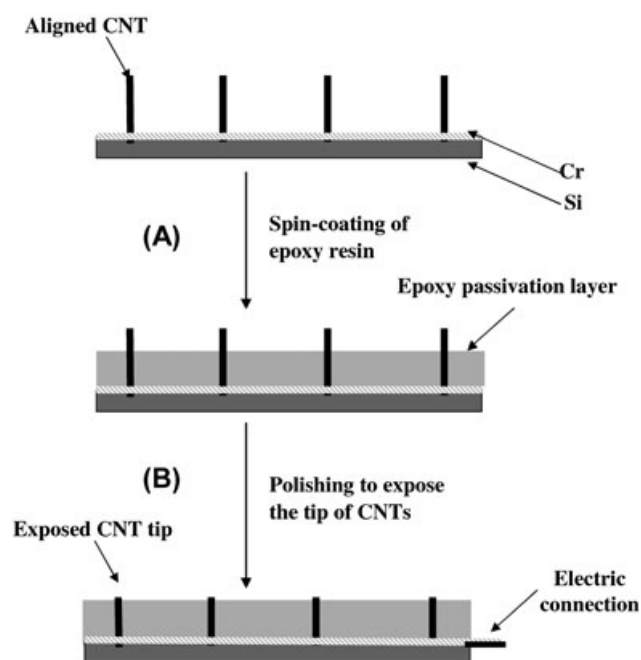


Fig. 2. Fabrication scheme of the CNT nanoelectrode arrays. A) Spin-coating of epoxy resin as passivation layer; B) polishing to expose the tip of CNTs

$10^6 - 3 \times 10^6 / \text{cm}^2$ , a length of 10–12 μm, and a diameter of 50–80 nm. Figure 1 shows the SEM image of aligned CNT arrays with site density of  $2 \times 10^6 \text{ cm}^{-2}$ .

Figure 2 shows the scheme of the fabrication procedure of NEAs after growth of aligned CNTs arrays. The Epon epoxy resin 828 was investigated as a potential spin-coating material for the passivation layer of our NEAs. A 2-gram quantity of the epoxy resin was weighed into a small glass vial and the vial placed into a 70 °C water bath. At this temperature, the viscosity of Epon 828 decreased dramatically but was still too high for the spin coating. A 2.5-mL volume of tetrahydrofuran (THF) was added to further reduce the viscosity of the resin. Then 0.28 grams (14 wt. %) of MPDA hardener was added to the stirred resin. After 2 to 3 minutes, 0.15 mL of the epoxy mixture was dropped on the aligned CNTs on the Si substrate. The CNTs substrate was preheated on a hot plate at 70 °C to maintain the viscosity of the epoxy mixture after it was dropped on the substrate. Then the substrate was quickly transferred to a spin-coater and spun at 7000 rpm for 1 minute. The aligned CNTs showed very good mechanical properties; they were maintained in vertical alignment after the resin-dropping and spin-coating processes. The sample was left in room temperature for one day, then heated (cured) in an oven at 90 °C for 1 hour, followed by a post cure at 150 °C for 1 to 2 days [27]. After the curing processes, a uniform thin layer of epoxy resin (7–9 μm) was obtained on the substrate. The CNTs were half embedded in the resin with 2 to 3 μm protruding out. By using a lens paper to gently polish the sample, the protruding part of CNTs were broken and removed by ultrasonication in water. Then the electrical connection was made on the CNT-Si substrate. Finally, the electrode arrays

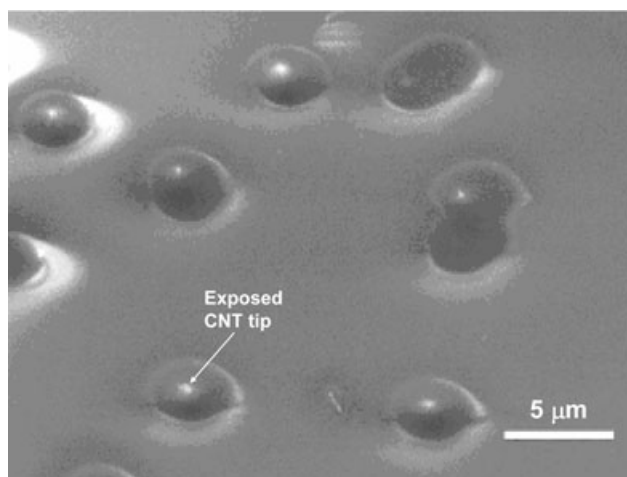


Fig. 3. SEM image of CNT nanoelectrode arrays fabricated from the low-site density CNTs arrays (after polishing). White dots are the exposed CNT tips.

were pretreated by electrochemical etching in 1.0 M NaOH at 1.5 V for 90 seconds [19] prior to the electrochemical characterizations. The final nanoelectrodes produced were carbon nanoelectrodes with a diameter of 50–80 nm (Figure 3). The CNTs-NEAs fabricated based on this design effectively use the open ends of CNTs for electrochemical sensing. The open ends of the CNTs have fast electron transfer rates similar to a graphite edge-plane electrode, while the side-walls present very slow electron transfer rates similar to the graphitic basal plane [28, 33].

### 2.3. Evaluation of the Carbon Nanotubes Nanoelectrode Arrays

Cyclic voltammetry (CV) of  $K_3Fe(CN)_6$  was used to evaluate the carbon nanotube nanoelectrode array. The experiments were performed with a PC4/750 Potentiostat electrochemical measurement system (Gamry Instruments, Inc.). A platinum wire was used as the counter electrode and saturated calomel electrode (SCE) as the reference electrode. Square-wave voltammetry (SWV) of the carbon nanotubes NEAs were examined to evaluate the potential applicability in quantitative analysis by using CHI 1232 electrochemical analyzer (CH Instrument, Austin, TX) with platinum wire as the count electrode and Ag/AgCl as the reference electrode. All solutions were degassed for a few minutes by passing through  $N_2$  gas.

### 2.4. Detection of $Pb^{2+}$ Using Square-Wave Stripping Voltammetry

Square-wave voltammetric analysis of  $Pb^{2+}$  was performed on the CHI 1232 electrochemical analyzer. All solutions were degassed for a few minutes by passing through  $N_2$  gas. In the stripping analysis, the CNT-NEAs were deposited with Hg before the detection of  $Pb^{2+}$  using the conditions of:

5 ppm  $Hg^{2+}$  in 0.1 M  $NaNO_3$ , and a potential of  $-1.1$  V applied for a 5 minute period. Then the electrodes were rinsed with ultra pure water. The detection of  $Pb^{2+}$  was a two-step process. The first step was the electrodeposition of  $Pb^{2+}$  onto the nanoelectrodes, a negative potential of  $-1.1$  V was applied to the electrodes that were immersed in  $Pb^{2+}$  solutions with 0.1 M  $NaNO_3$  as supporting electrolyte for a specified period of time (e.g., 1 to 10 minutes) under the stirred conditions, followed by a 10 second quiet period. In the detection step, the potential was scanned from  $-1.1$  V to  $-0.1$  V in the same solution under quiet conditions. The response peak of lead appeared at  $-0.45$  V (vs. Ag/AgCl). Once the Hg film was deposited on the CNTs-NEAs, the electrode arrays can be used to detect the  $Pb^{2+}$  solutions with varied concentrations (incrementally from 2 to 100 ppb) or varied deposition periods without redeposition of Hg film and surface regeneration.

## 3. Results and Discussion

### 3.1. Cyclic Voltammetry of the Carbon Nanotubes Nanoelectrode Arrays

Figure 4a shows the cyclic voltammogram of the NEAs in 4 mM  $K_3Fe(CN)_6/0.5$  M  $KNO_3$  solution at a scan rate of 20 mV/s. The sigmoidal voltammogram is a sign of microelectrode behavior (radial diffusion). The steady-state current arises because the electrolysis rate is approximately equal to the rate of diffusion of analyte to the electrode surface [29]. Figure 4b shows the scan rate analysis of the NEAs. The scan-rate-independent limiting current behavior up to 500 mV/s was observed on the nanoelectrode array, which indicated that there is no diffusion layer overlap between the electrodes under this condition. This is because most of the CNTs on the NEAs are separated from their nearest neighbor for at least 5 μm, much larger than the diameter of each nanotube (50 to 80 nm). The ratio of the inter-electrode distance ( $d$ ) to the electrode radius ( $r$ ) is much larger than 40, which satisfies the conditions for the electrode array to produce sigmoidal shape voltammogram even at high scan rate [23, 24]. The peak shaped voltammograms were not observed until 2000 mV/s. This enables high-speed detections of analytes and investigations of redox processes having fast kinetics.

It is well recognized that nanoelectrode has dramatically lower capacitive current than conventional macroelectrodes [30–32], which was also observed in our NEAs. Capacitive current ( $I_c$ ), the main cause of the background in voltammetry, is proportional to the active electrode area ( $A_{act}$ ), scan rate ( $\nu$ ), and capacitance ( $C_d$ );  $I_c = A_{act}\nu C_d$  [31]. Reducing the capacitive current can greatly improve the signal to noise ratio. As shown in Figure 2a, the forward and reverse scan curves are almost identical, which indicates very low capacitive current. The low capacitance is attributed to the very small electrode size, it also resulted from the spin coated epoxy film, both the material itself and the layer quality [21, 29, 30]. Beside, the good sealing provided by the

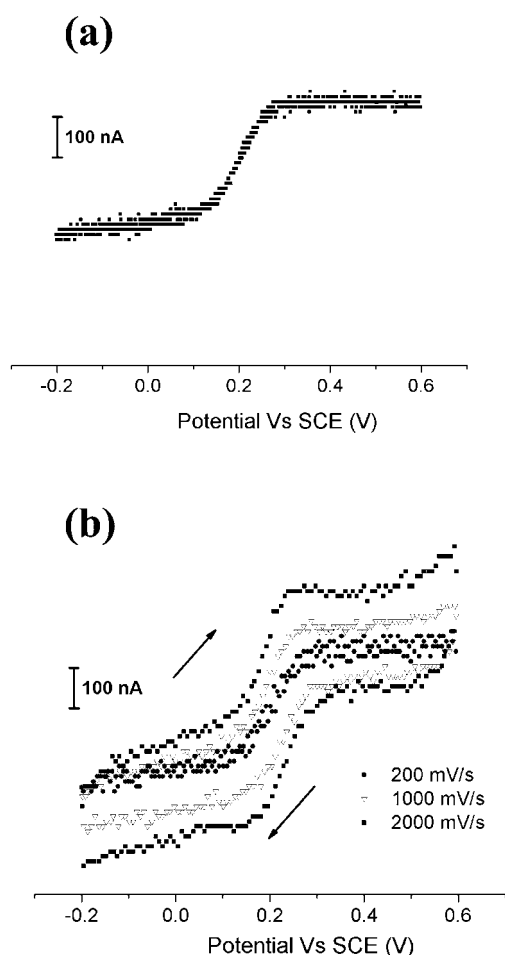


Fig. 4. Cyclic voltammograms of the carbon nanotubes nanoelectrode array in 4 mM  $K_3Fe(CN)_6/0.5$  M  $KNO_3$  solution at the scan rate of a) 20 mV/s, b) 200–2000 mV/s.

spin coated epoxy film leads to very low current leakage flowing to the electrode back contact, which can be seen from the flat baseline in the CV curve. At high scan rates as shown in Figure 4b, the capacitive current increases with the increasing scan rate, causing more noticeable separation between forward and reverse scans. Lifetime of the NEAs was significantly improved: there was no degradation for several weeks, which is attributed to the excellent stability of the epoxy layer. With proper cure, Epon resin 828 shows excellent mechanical, adhesive, dielectric, and chemical resistant properties. It had been used to coat the carbon micro fibers in the fabrication of carbon-fiber-based micro-electrodes [27]. Our experiments demonstrate that Epon resin 828 can also be used as a spin-coating material for the fabrication of nanoelectrode arrays.

### 3.2. Square-Wave Voltammetry of the Carbon Nanotubes Nanoelectrode Arrays

For analytical applications, SWV have advantages in providing the highest sensitivity among electroanalytical

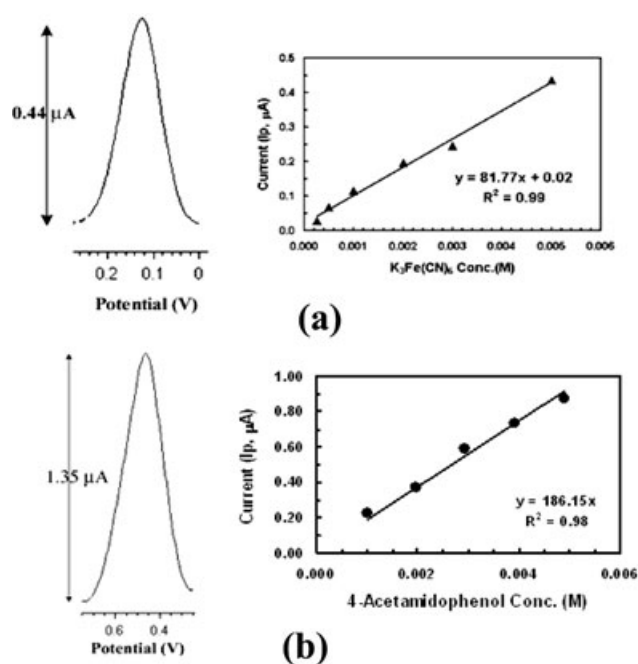


Fig. 5. Representative square-wave voltammograms of the CNT nanoelectrode array in a) 5 mM  $K_3Fe(CN)_6$  in 0.2 M  $KNO_3$  solution, and b) 10 mM 4-acetamidophenol in 0.2 M  $KNO_3$  solution and their calibration plots. Pulse amplitude, 25 mV; step amplitude, 5 mV; frequency, 100 Hz.

techniques by the ability to subtract the double-layer charging current [28]. Figure 5a shows the square-wave voltammogram of 5 mM  $K_3Fe(CN)_6$  in 0.2 M  $KNO_3$  solution and the calibration plot. Figure 5b shows the square-wave voltammogram of 10 mM 4-acetamidophenol in 0.2 M  $KNO_3$  solution and the calibration plot. Both voltammograms show a well-defined peak shape where the anodic peaks of  $K_3Fe(CN)_6$  and 4-acetamidophenol are found at 0.12 V and 0.45 V, respectively. The peak currents are proportional to the analyte concentration in the solution. These results indicate the feasibility of using the CNT-NEAs as a general platform for sensitive electrochemical sensing of electroactive analytes using SWV.

### 3.3. Stripping Voltammetric Detection of $Pb^{2+}$

Lead is increasingly found in drinking water in many parts of the world stemming from industrial processes as well as geochemical mechanisms, it is regarded as highly toxic metal ions to a wide variety of organs in both humans and animals, including nervous, immune, reproductive, gastrointestinal systems. The ability to rapidly detect a trace amount of  $Pb^{2+}$  species on-site is very desirable. The feasibility of using CNT-NEAs for stripping voltammetric detection of toxic lead(II) had also been evaluated. Figure 6a shows the effect of deposition time of 5 ppb  $Pb^{2+}$  in 0.1 M  $NaNO_3$  solution, the voltammetric response (current) of lead is a linear function of the deposition time ranging for 1 to 10 minutes. In Figure 6b, the right inset is the response peaks of 2 to

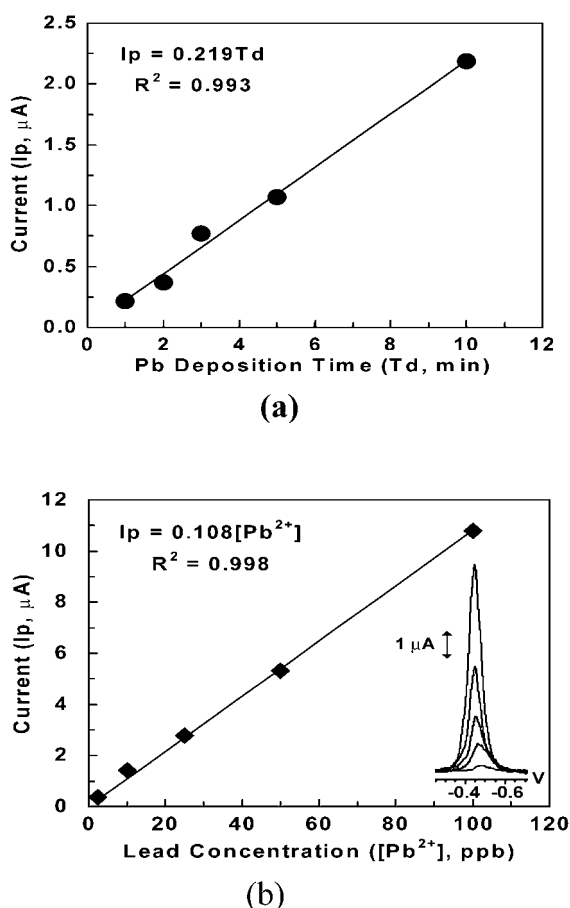


Fig. 6. The voltammetric response (current) of  $\text{Pb}^{2+}$  in 0.1 M  $\text{NaNO}_3$  solution as a) a function of deposition time, measured with 5 ppb  $\text{Pb}^{2+}$ , and b) a function of  $\text{Pb}^{2+}$  concentration, measured after 3 minutes deposition. Pulse amplitude, 25 mV; step amplitude, 5 mV; frequency, 100 Hz. The voltammograms correspond to  $\text{Pb}^{2+}$  concentration of 2, 5, 25, 50, and 100 ppb.

100 ppb  $\text{Pb}^{2+}$  after 3 minutes of deposition, it can be seen that the voltammetric response is a linear function of  $\text{Pb}^{2+}$  concentrations ranging from 2 to 100 ppb. At 25 ppb  $\text{Pb}^{2+}$  and 3 minutes deposition time, the average response (current) was 2.78  $\mu\text{A}$ , and the % RSD was 2.75 ( $n = 5$ ). Detection limit of  $\text{Pb}^{2+}$  was 1 ppb after a 3-min preconcentration period.

The effect of electrolyte concentration on SW stripping analysis was also evaluated with CNTs-NEAs and glassy carbon (GC) electrode (3 mm i.d.). At 0.1 M  $\text{NaNO}_3$  electrolyte solution, well-defined voltammograms for  $\text{Pb}^{2+}$  were obtained for both the NEAs and GC electrode. The current ratio of GC/NEAs was about 10 for 100 ppb  $\text{Pb}^{2+}$  in 0.1 M  $\text{NaNO}_3$  electrolyte solution. When electrolyte concentration decreased to  $10^{-4}$  M  $\text{NaNO}_3$ , the peak-shape of  $\text{Pb}^{2+}$  in the voltammograms obtained with the CNTs-NEAs was still well-defined, whereas the peak-shape in the voltammograms obtained with GC electrode was distorted and peak current decreased significantly. The small size of the total electrode surface of the CNT-NEAs resulted in a much smaller current ( $i$ ) than that obtained by the GC

electrode. Ohmic drops ( $-iR$ ) as a result of current flowing through solution generates a potential that opposes the applied potential. For the CNT-NEAs, since the current ( $i$ ) was relatively small, the ohmic drop was not large even at large resistance ( $R$ ) in the highly resistive solutions (i.e., aqueous solution with extremely low concentration electrolyte). This allows the CNT-NEAs to be operated under very low electrolyte conditions. Low electrolyte conditions are often desirable because [34]: 1) high ionic strength can affect the activities and the mobilities of ions, 2) the interactions between the supporting electrolyte and the analyte can be significant and undesirable, 3) adding supporting electrolyte is time-consuming and may introduce impurities.

#### 4. Conclusions

In summary, we described a novel fabrication process of carbon nanotubes nanoelectrode arrays. The carbon nanotubes nanoelectrode arrays provided an excellent platform for electroanalysis. Cyclic voltammetry showed the sigmoidal shape with low capacitive current and scan-rate-independent limiting current. The results of square-wave voltammetry indicated the feasibility of using CNTs-NEAs for voltammetric detection of electroactive analytes. The CNT-NEAs were used successfully for voltammetric detection of trace amounts of lead(II) at the ppb level. Insignificant ohmic drop due to the small current at the CNT-NEAs allowed the electrode arrays to be less affected by high solution resistance in very low electrolyte conditions than the glassy carbon electrode.

#### 5. Acknowledgements

This work performed at Boston College was partially supported by DOE (DE-FG02-00ER45805) and partially by NSF (CMS-0219836). The work performed at Pacific Northwest National Laboratory (PNNL) was supported by DOE-EMSP and NIH/1R01 ES010976-01A2. The research described in this paper was performed in part at the Environmental Molecular Sciences Laboratory (EMSL), a national scientific user facility sponsored by the DOE's Office of Biological and Environmental Research and located at PNNL. PNNL is operated by Battelle Memorial Institute for the U.S. Department of Energy (DOE).

#### 6. References

- [1] Y. Lin, W. Yantasee, F. Lu, J. Wang, M. Musameh, Y. Tu, Z. F. Ren, *Biosensors Based on Carbon Nanotubes* in *Dekker Encyclopedia of Nanoscience and Nanotechnology* (Eds: J. A. Schwarz, C. Contescu, K. Putye), Marcel Dekker, New York **2004**, pp. 361–374.
- [2] P. J. Britto, K. S. V. Santhanam, P. M. Ajayan, *Bioelectrochem. Bioenerg.* **1996**, *41*, 121.
- [3] G. Che, B. B. Lakshmi, E. R. Fisher, C. R. Martin, *Nature* **1998**, *393*, 346.

- [4] P. J. Britto, K. S. V. Santhanam, A. Rubio, A. J. Alonso, P. M. Ajayan, *Adv. Mater.* **1999**, *11*, 154.
- [5] J. Li, A. Cassell, L. Delzeit, J. Han, M. Meyyappan, *J. Phys. Chem. B* **2002**, *106*, 9299.
- [6] J. M. Nugent, K. S. V. Santhanam, A. Rubio, P. M. Ajayan, *Nano Lett.* **2001**, *1*, 87.
- [7] J. Wang, M. Musameh, Y. Lin, *J. Am. Chem. Soc.* **2003**, *125*, 2408.
- [8] H. Luo, Z. Shi, N. Li, Z. Gu, Q. Zhuang, *Anal. Chem.* **2001**, *73*, 915.
- [9] J. K. Campbell, L. Sun, R. M. Crooks, *J. Am. Chem. Soc.* **1999**, *121*, 3779.
- [10] M. Musameh, J. Wang, A. Merkoci, Y. Lin, *Electrochem. Commun.* **2002**, *4*, 743.
- [11] Y. Lin, S. Taylor, H. P. Li, K. A. Fernando, L. W. Qu, W. Wang, L. R. Gu, B. Zhou, Y. P. Sun, *J. Mater. Chem.* **2004**, *14*, 527.
- [12] J. J. Davis, R. J. Coles, H. A. O. Hill, *J. Electroanal. Chem.* **1997**, *440*, 279.
- [13] R. J. Chen, Y. G. Zhang, D. W. Wang, H. J. Dai, *J. Am. Chem. Soc.* **2001**, *123*, 3838.
- [14] B. R. Azamian, J. J. Davis, K. S. Coleman, C. B. Bagshaw, M. L. H. Green, *J. Am. Chem. Soc.* **2002**, *124*, 12664.
- [15] C. V. Nguyen, L. Delzeit, A. M. Cassell, J. Li, J. Han, M. Meyyappan, *Nano Lett.* **2002**, *2*, 1079.
- [16] Y. Lin, F. Lu, J. Wang, *Electroanalysis* **2004**, *16*, 145.
- [17] Y. Tu, Y. Lin, Z. F. Ren, *Nano Lett.* **2003**, *3*, 107.
- [18] M. A. Guillorn, T. E. McKnight, A. Melechko, V. I. Merkulov, P. F. Britt, D. W. Austin, D. H. Lowndes, M. L. Simpson, *J. Appl. Phys.* **2002**, *91*, 3824.
- [19] J. Li, H. T. Ng, A. Cassell, W. Fan, H. Chen, Q. Ye, J. Koehne, J. Han, M. Meyyappan, *Nano Lett.* **2003**, *3*, 597.
- [20] R. Feeney, S. P. Kounaves, *Electroanalysis* **2000**, *12*, 677.
- [21] S. Fletcher, M. D. Horne, *Electrochem. Commun.* **1999**, *1*, 502.
- [22] M. E. Sandison, N. Anicet, A. Glidle, J. M. Cooper, *Anal. Chem.* **2002**, *74*, 5717.
- [23] H. J. Lee, C. Beriet, R. Ferrigno, H. H. Girault, *J. Electroanal. Chem.* **2001**, *502*, 138.
- [24] F. Fassbender, G. Schmitt, M. J. Schoning, H. Luth, G. Buss, J. W. Schultze, *Sens. Actuators B* **2000**, *68*, 128.
- [25] X. Yu, D. Chattopadhyay, I. Galeska, F. Papadimitrakopoulos, J. F. Rusling, *Electrochem. Commun.* **2003**, *5*, 408.
- [26] Y. Tu, Z. P. Huang, D. Z. Wang, J. G. Wen, Z. F. Ren, *Appl. Phys. Lett.* **2002**, *80*, 4018.
- [27] A. C. Michael, R. M. Wightman, in *Laboratory Techniques in Electroanalytical Chemistry* (Eds: P. T. Kissinger, W. R. Heineman), Marcel Dekker, New York **1996**, pp. 368–371.
- [28] R. L. McCreery, K. K. Cline, in *Laboratory Techniques in Electroanalytical Chemistry* (Eds: P. T. Kissinger, W. R. Heineman), Marcel Dekker, New York **1996**, pp. 299–301.
- [29] K. R. Wehmeyer, R. M. Wightman, *J. Electroanal. Chem.* **1985**, *196*, 417.
- [30] V. P. Menon, C. R. Martin, *Anal. Chem.* **1995**, *67*, 1920.
- [31] P. Ugo, L. M. Moretto, F. Veza, *Chem. Phys. Chem.* **2002**, *3*, 917.
- [32] D. Pletcher, in *Microelectrode: Theory and Applications* (Eds: M. I. Montenegro, M. A. Queiros, J. L. Daschbach), NATO ASI Series E, 197; Kluwer Academic Publishers, Boston **1990**; pp. 3–15.
- [33] J. Koehne, J. Li, A. M. Cassell, H. Chen, Q. Ye, H. T. Ng, J. Han, M. Meyyappan, *J. Mater. Chem.* **2004**, *14*, 676.
- [34] M. Ciszowska, Z. Stojek, *Anal. Chem.* **2000**, *72*, 754A.